JOM, Vol. 66, No. 8, 2014
DOI: 10.1007/s11837-014-1001-4

Direct Numerical Simulation of Solid Deformation During Dendritic Solidification

M. YAMAGUCHI[1] and C. BECKERMANN[1,2]

1.—Department of Mechanical and Industrial Engineering, University of Iowa, Iowa City, IA 52242, USA. 2.—e-mail: becker@engineering.uiowa.edu

Deformation of the semisolid mush during solidification is a common phenomenon in metal casting and can lead to defects such as hot tears, macrosegregation, and porosity. The morphology of the solidifying mush, including the shape of the dendrites and the distribution of grain boundaries, plays a key role in determining its mechanical behavior. In the current study, a polycrystalline phase-field model is combined with a material point method stress analysis to numerically simulate the fully coupled dendritic solidification and elasto-viscoplastic deformation behavior of a pure substance in two dimensions. It is shown that solid compressive and shear deformations result in variations in the crystallographic orientation angle within a single dendrite that, in turn, affect the subsequent solidification behavior. Shearing of a dendritic structure occurs primarily in relatively narrow bands near or inside the grain boundaries or the thin junctions between different dendrite arms. The deformations can cause the formation of low-angle tilt grain boundaries inside of individual dendrite arms. In addition, grain boundaries form when different arms of a deformed single dendrite impinge. During compression of a high-solid-fraction dendritic structure, the deformations are limited to a relatively thin layer along the compressing boundary. The compression causes consolidation of this layer into a fully solid structure that consists of numerous subgrains.

INTRODUCTION

Deformation of the solid is a common occurrence during metal casting processes.[1,2] Often, the solid deforms simply due to thermal stresses, but sometimes the deformation is caused by external forces, for example through the rolls in continuous casting, mold wall movement, or an applied pressure. When the casting is still solidifying, the deformations can extend into the semisolid mushy zone. This mushy zone is typically composed of solid dendrites surrounded by liquid. Deformation of the mush can lead to numerous defects in a solidified casting, including hot tears, macrosegregation, and porosity. Therefore, understanding the mechanical behavior of the mush is of great interest for advancing casting simulations incorporating a stress analysis[3] and, ultimately, for preventing defects in castings.

In the current study, a numerical method is developed for simulating the deformation of a solidifying mush on the scale of the evolving microstructure. Such direct numerical simulations may lead to improved constitutive models for use in macroscopic stress simulations. Mush deformation is a complex process involving multiple physical phenomena: solidification and formation of bridges or grain boundaries between dendrites, large inelastic solid deformation with contacts, liquid flow, *etc*. Simulating all of these processes simultaneously would be a very challenging task. A few researchers have developed models to investigate the mechanical behavior of mush. Phillion et al.[4] and Fuloria and Lee[5] calculated inelastic deformation of multigrain and dendritic microstructures, respectively, without considering solidification. Uehara et al.[6] performed thermal stress simulations in a confined solidifying microstructure. Fully coupled solidification and deformation simulations of dendritic microstructures have not been performed in the past. The coupling of the solidification and deformation calculations is important not only because the deformations are a function of the

(Published online June 17, 2014)

morphology of the evolving solid but also because the solidification patterns are affected by the deformations.

Grain boundaries play an important role in the deformation of a mush, especially at high volume fractions of solid. For example, they can delay the formation of solid bridges between dendrites. Not surprisingly, hot tears due to tensile strains in a mushy zone usually form at grain boundaries.[7,8] Although Phillion et al.[4] simulated deformation of multiple grains, they did not consider the dynamics of grain boundaries. Sistaninia et al.[9] developed a three-dimensional (3-D) granular model to study the mechanical behavior of a semisolid mush at high fractions of solid. Although solidification of the initial grain structure was simulated in Ref. [9], the subsequent stress analysis was uncoupled. Clearly, the microstructure of the solid plays a key role in the mechanical behavior of a mush. But solid deformations can also affect the evolution of the solid morphology by solidification and grain boundary dynamics. For example, a new grain boundary can form when a severely deformed dendrite arm grows into an undeformed portion of the same dendrite. New tilt grain boundaries can form when a dendrite arm is bent.

This article summarizes the research originally presented by the authors in Refs. [10], [11], highlights potential shortcomings, and points out the areas where additional developments are needed. The reader is referred to these references for the governing equations, the numerical procedures and settings, and the validation of the simulation results.

MODEL DESCRIPTION

To simplify the problem, the current study focuses on dendritic solidification and elasto-viscoplastic deformation of a pure substance in two dimensions. Stresses that are exerted by the liquid on the solid are neglected. This assumption is realistic when the liquid can "drain" freely. In fact, the flow of the liquid is not modeled at all. Transformation stresses/strains, stress-induced phase transformations, and heat generation due to inelastic deformation are not considered. These assumptions are all appropriate for a slowly deforming mush.

The simulation of dendritic solidification with large solid deformations necessitates numerous choices regarding the models to be used and the numerical methods to be employed. Solidification, including the presence of multiple crystals with different crystallographic orientations, and the formation and motion of grain boundaries is simulated in the current study using the polycrystalline phase-field model of Warren et al.[12] Because the phase-field method employs a diffuse interface concept, it is especially well suited for handling morphological changes and singularities, such as those caused by portions of a dendrite impinging on one another. Such wetting and bridging phenomena are not well handled by traditional sharp interface approaches. As in all phase-field models, the phase-field parameter ϕ is used to indicate the local crystalline order, with $\phi = \pm 1$ inside of the bulk solid and liquid phases, respectively. The solid–liquid interface is treated as a diffuse layer of small but finite thickness over which the phase field varies smoothly between $\phi = \pm 1$. The grain boundary between two solid grains is also treated as a diffuse interface. Because the crystalline order inside of a grain boundary is reduced, the phase field assumes values below unity (solid) within the grain boundary. An additional order parameter, the crystal orientation angle field α is introduced to measure the local crystallographic orientation of the solid with respect to a fixed coordinate system. If two neighboring grains are misoriented, then the orientation angle varies smoothly across the diffuse grain boundary from the value in one grain to the value in the other grain. The misorientation $\Delta\alpha$ is given by the integral of the orientation angle gradient $\nabla\alpha$ across the grain boundary. The phase field and the orientation angle are closely coupled inside of a grain boundary. The larger the angle gradient (or misorientation), the lower the minimum value of the phase field. At some critical misorientation, the minimum value of the phase field reaches $\phi = -1$ and the grain boundary is fully wet. The model of Warren et al.[12] also considers the anisotropy in the interfacial energy, which is essential for modeling dendritic solidification. They demonstrated that the model correctly predicts phenomena such as triple junction behavior, the wetting condition for a grain boundary, curvature-driven grain boundary motion, and grain rotation. The main new feature of the current phase-field calculations is that because of the deformation of the solid, the crystallographic orientation angle is no longer uniform within a single dendrite and continuously evolves. Furthermore, the phase field and the temperature field are advected by the deformation velocity.

The stress model for simulating the elasto-viscoplastic deformation of the solid assumes that the solid–liquid interface is sharp. The zero contour line of the phase field is used to identify the interface. The stress model is solved only in the solid and the solid–liquid interface is taken as stress free. The numerical method employed in the solution of the stress model needs to be able to handle large strains, self-contact, and impingement of solid. Particle methods or meshless methods are attractive for this purpose because they do not suffer from the mesh collapse or entanglement problems typical of Lagrangian finite-element methods. In the current study, the material point method[13] is selected. The main feature of this method is that it uses, as in a particle method, a Lagrangian description for the motion of material points, and a fixed Eulerian background mesh for solving the equation of motion. The latter feature makes the material point method

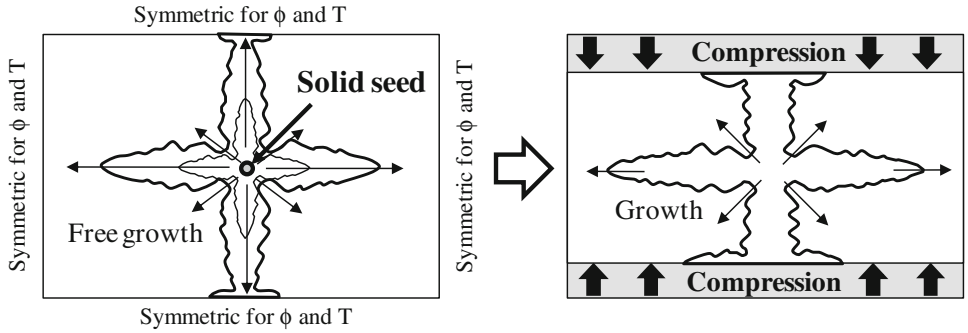

Fig. 1. Schematic of the computational setup for the simulation of the compression of a single dendrite.

well suited for coupling with the (Eulerian) phase-field method.

Special consideration must be given to the mechanical behavior of a grain boundary. It is known that the strength of low-angle grain boundaries ($\Delta\alpha$ less than about 11°) decreases with increasing misorientation between the grains. For high-angle grain boundaries ($\Delta\alpha$ greater than about 11°), the bonds between the grains are weakened further, but the properties are normally unrelated to the misorientation. In both cases, the reductions in the strength can be attributed to the reduced crystalline order inside of a grain boundary. Above a certain critical misorientation $\Delta\alpha_c$, the grain boundary is wet and has no strength. The crystals separated by a wet grain boundary would be able to slide against each other and could be pulled apart easily. Based on these considerations, the local mechanical properties inside of a grain boundary may be related directly to the value of the phase field ϕ because it is a measure of the local crystalline order. Recall that inside of a grain boundary, the phase field assumes values below unity. However, quantitative relations between mechanical properties, such as the elastic modulus or the yield strength, and the value of the phase field inside of a grain boundary are currently not available. Therefore, a highly simplified procedure is adopted in the current study to model these effects. When the value of the phase field is greater than zero ($\phi > 0$), the material inside of a grain boundary is assumed to behave mechanically like a solid, and material points are assigned to that computational cell in the material point method stress analysis. Hence, a grain boundary becomes mechanically bridged (by solid) as soon as the minimum value of the phase field inside of the grain boundary exceeds zero. Conversely, for $\phi < 0$ the material is treated in the stress analysis as a liquid. In other words, a grain boundary is assumed to behave mechanically like a liquid when the minimum value of the phase field inside of the grain boundary is below zero, even though it is not fully wetted until the minimum value reaches $\phi = -1$. In the presence of liquid-like material ($-1 < \phi < 0$) inside of a grain boundary, no stresses are transmitted between the two crystals because the stress model is solved only in cells that are solid and the stresses in the liquid are not calculated (i.e., they are zero). Clearly, a more sophisticated model should be developed that solves for the stresses not only in the solid but also in the liquid. Such a model could incorporate phase-field-dependent mechanical properties reflecting the weakening of the solid due to reduced crystalline order inside of a grain boundary.

RESULTS AND DISCUSSION

Compression of a Single Dendrite

An initial simulation is performed of the compression of a single dendrite without considering the formation of grain boundaries. As illustrated in Fig. 1, the dendrite is compressed in a rectangular domain that is bounded by adiabatic walls. Initially, the domain contains an undercooled liquid, except for a solid seed at the center. The seed grows freely into the undercooled melt and develops into a dendrite. Once the vertical dendrite arms reach the top and bottom walls, the walls start to move inward at a prescribed rate. This imposes a compression loading on the growing dendrite. In order for some solidification to occur during the compression, the displacement rate of the top and bottom walls was chosen to be approximately equal to the dendrite tip growth velocity. This can be best observed in Fig. 2 below by the movement of the tips of the horizontally growing dendrite arms relative to the changes in the position of the top and bottom walls. The mechanical properties for the solid dendrite were chosen to approximately represent the mechanical properties of metals near the melting point.[3]

The results of the initial simulation are shown in Fig. 2. The rows of plots represent results at four different times corresponding to when the vertical dendrite arms have just touched the top and bottom walls, 10% compression, 20% compression, and 30% compression. The phase-field contours in the upper left corner of Fig. 2 indicate that before compression is initiated, the dendrite has a relatively slender shape with small sidebranches. At 10% compression, the phase-field contours (left column) and the equivalent plastic strain fields (center right column)

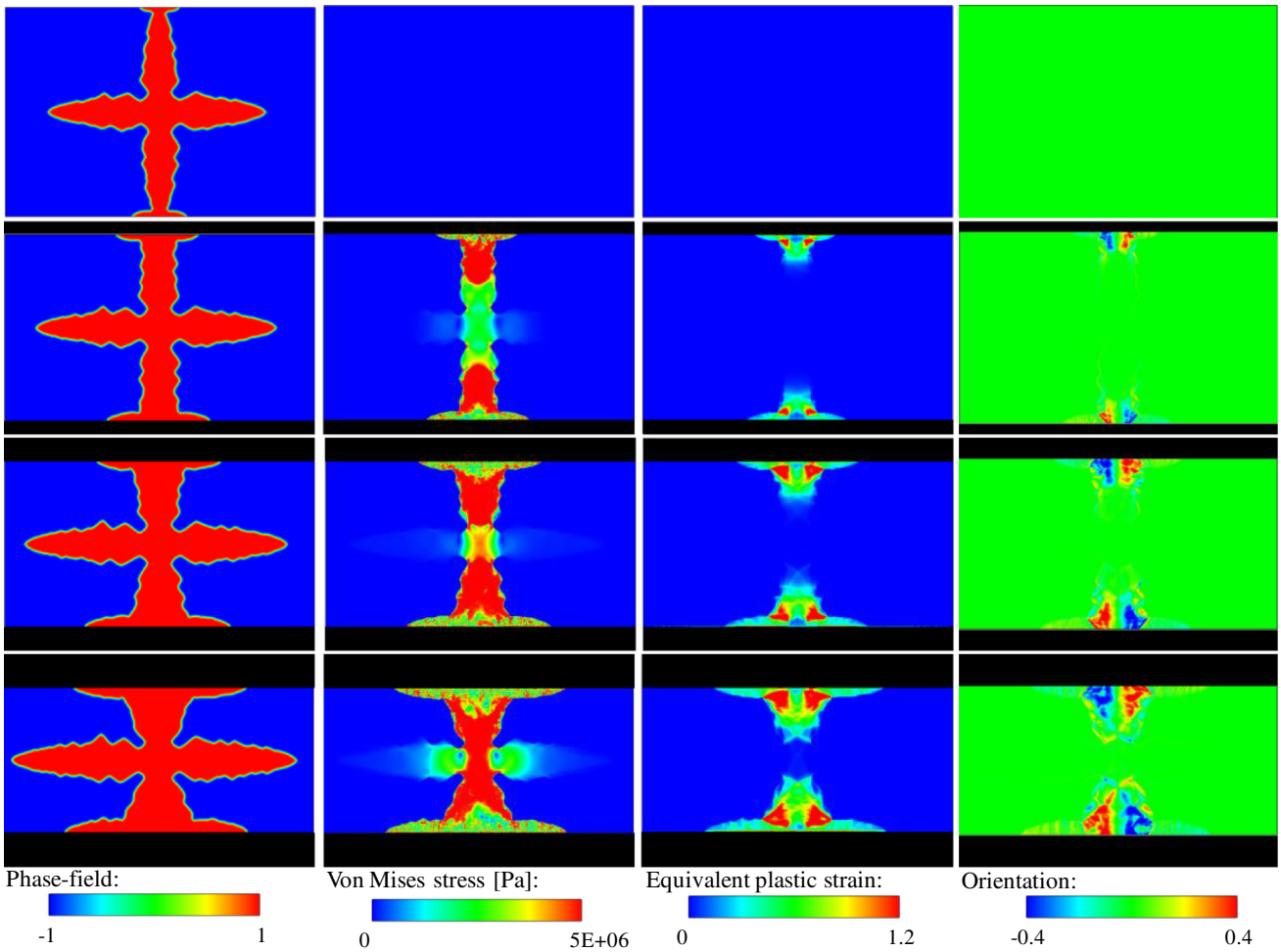

Fig. 2. Predicted phase field (left column), von Mises stress (center left column), equivalent plastic strain (center right column), and crystallographic orientation angle relative to an arbitrary coordinate system (right column) contours for elasto-perfectly plastic compression of a single dendrite growing into an undercooled melt. The results are shown for when the vertically growing dendrite tips just touched the walls and compression is initiated (first row), at 10% compression (second row), at 20% compression (third row), and at 30% compression (fourth row).

indicate that the deformation of the dendrite is still limited to the vertical growing dendrite arms near the top and bottom moving walls. In these portions of the dendrite, the yield stress of 5 MPa is reached and plastic strains in excess of 100% can be observed. As expected, the shape of the horizontally growing dendrite arms is unaffected by the compression. With increasing compression, the regions in the vertically growing dendrite arms that exhibit plastic deformation extend further toward the center of the dendrite. Furthermore, the (elastic) stresses in the center portion of the dendrite continually increase. Small stress concentrations become apparent in the valleys between the sidebranches and at the necks between the vertically growing arms and the dendrite core. At 20% compression (third row in Fig. 2), the center portion of the dendrite is starting to yield. At 30% compression (last row in Fig. 2), elastic stresses propagate even into the uncompressed horizontally growing dendrite arms. Because of the movement of the top and bottom walls, a large amount of solid mass is advected inward and the vertically growing dendrite arms are much thicker than without compression. The predicted evolution of the crystallographic orientation angle field is shown in the rightmost column of Fig. 2. Bending of the dendrite occurs primarily in a thin layer at the edges of the regions with large plastic deformations, while the center portions of the vertically growing dendrite arms do not experience any crystallographic angle changes due to symmetry. These results clearly illustrate that solid deformation can induce a nonuniform crystallographic orientation angle field within a single dendrite.

Shearing of a Dendritic Crystal

In the second example, shearing of a dendritic structure is simulated, including the formation and motion of grain boundaries. Initially, undercooled melt is contained in a rectangular domain that has adiabatic boundaries. Three solid seeds having the same crystallographic orientation ($\alpha = 0$) are placed

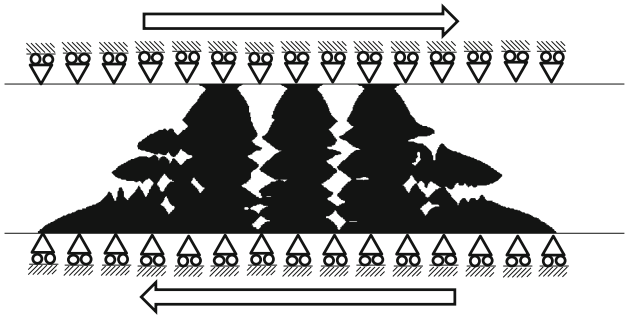

Fig. 3. Mechanical boundary conditions for the simulation of coupled solidification and shear deformation of a dendritic structure.

along the bottom wall. As shown in Fig. 3, the seeds evolve into a complex dendritic structure with numerous relatively slender sidearms. The dendritic structure is a single crystal because the orientation angle is the same everywhere (see Fig. 4b below). Shearing is initiated when the solid reaches the upper wall of the domain. The shearing is accomplished by translating the upper and lower domain walls to the right and left, respectively, as illustrated in Fig. 3. The (constant) translation speed is chosen low enough that considerable additional solidification occurs during the shearing.

The three rows of panels in Fig. 4 show the computed phase field and crystallographic orientation

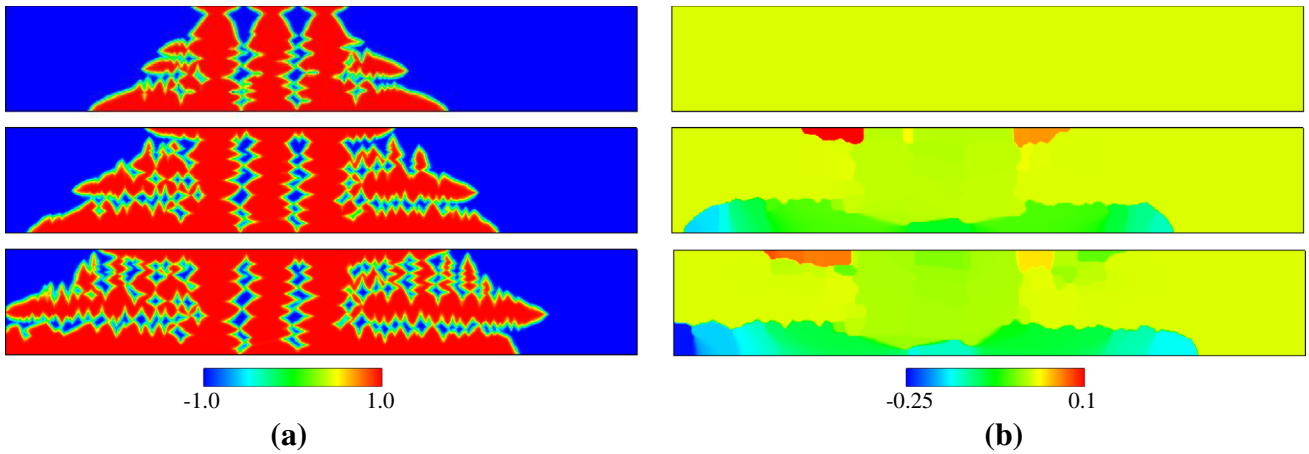

Fig. 4. Computed phase field (a) and crystallographic orientation angle (b) contours during solidification and shear deformation of a dendritic crystal. From top to bottom, the rows of plots correspond to 0%, 15%, and 30% shear.

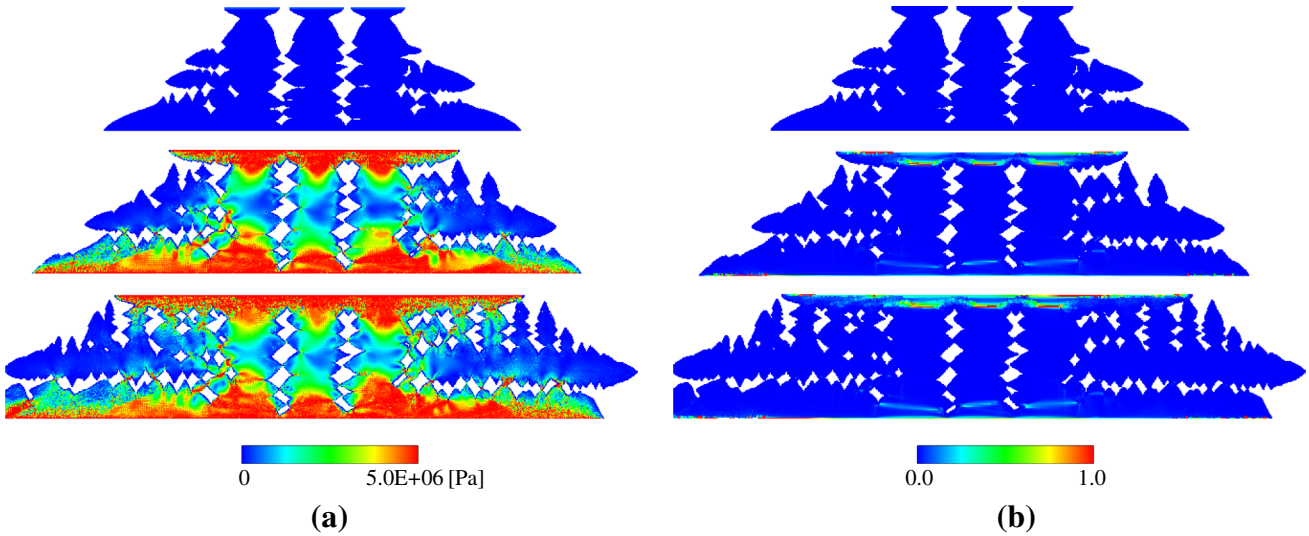

Fig. 5. Computed von Mises stress (a) and equivalent plastic strain (b) contours in the solid during solidification and shear deformation of a dendritic crystal. From top to bottom, the rows of plots correspond to 0%, 15%, and 30% shear.

angle contours at 0%, 15%, and 30% shear. A 15% (30%) shear implies a translation of both the upper and lower walls by an amount equal to 15% (30%) of the height of the domain. The corresponding von Mises stress and equivalent plastic strain contours in the solid are displayed in Fig. 5. At 15% shear, the continuous layers of solid along the upper and lower domain walls have reached the yield stress and are deforming plastically (Fig. 5). The plastic strain is mostly limited to horizontal shear bands at the relatively thin junctions between the three vertical dendrite arms and the solid layers along the horizontal walls. Several shear bands are also present in the solid directly adjacent to the moving horizontal walls. The stresses propagate into the three vertical dendrite arms, but most of the center portion of the dendrite does not yield. At 30% shear, the solid has continued to grow and deform, but the overall stress and plastic strain patterns are similar to the ones at 15% shear. Some of the higher order dendrite arms from the horizontally growing dendrite branches in the center of the domain are beginning to form bridges to the solid layers along the top and bottom walls. These very small bridges are also yielding. In general, the strain is localized in thin shear bands in the thin junctions between dendrite branches.

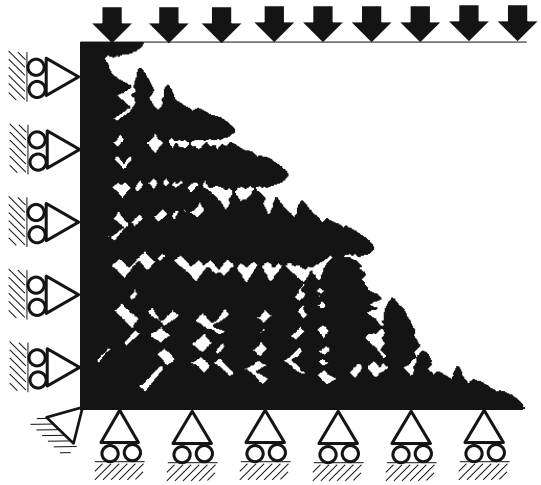

Fig. 6. Mechanical boundary conditions for the simulation of coupled solidification and compression of a dendritic network.

The computed deformations of the solid have a profound effect on the crystallographic orientation angle field in the dendrite, as displayed in Fig. 4b. The shearing causes several distinct subgrains to form within the solid layers along the top and bottom walls. The formation of the subgrain boundaries can be explained by the standard tilting mechanism. The subgrain boundaries in the solid layers along the top and bottom walls can all be characterized as low angle because the misorientations between the subgrains are always much below $\Delta\alpha \approx 0.2$ ($\approx 11°$). Furthermore, the values of the phase field inside of the subgrain boundaries remain very close to unity (Fig. 4a), implying that the solid layers along the top and bottom walls behave mechanically as a single solid structure. Over time, the subgrains undergo some coarsening, but the shearing continues to create new subgrains. High-angle grain boundaries can be observed between some of the subgrains in the solid layers and the horizontally growing dendrite branches in the center of the domain, which are essentially undistorted ($\alpha = 0$). Hence, in addition to the formation of tilt grain boundaries inside of individual dendrite arms, impingement of different arms of a deformed single dendrite can also lead to grain boundaries. While these phenomena are well known in the manufacture of single crystals, they have not been simulated previously.

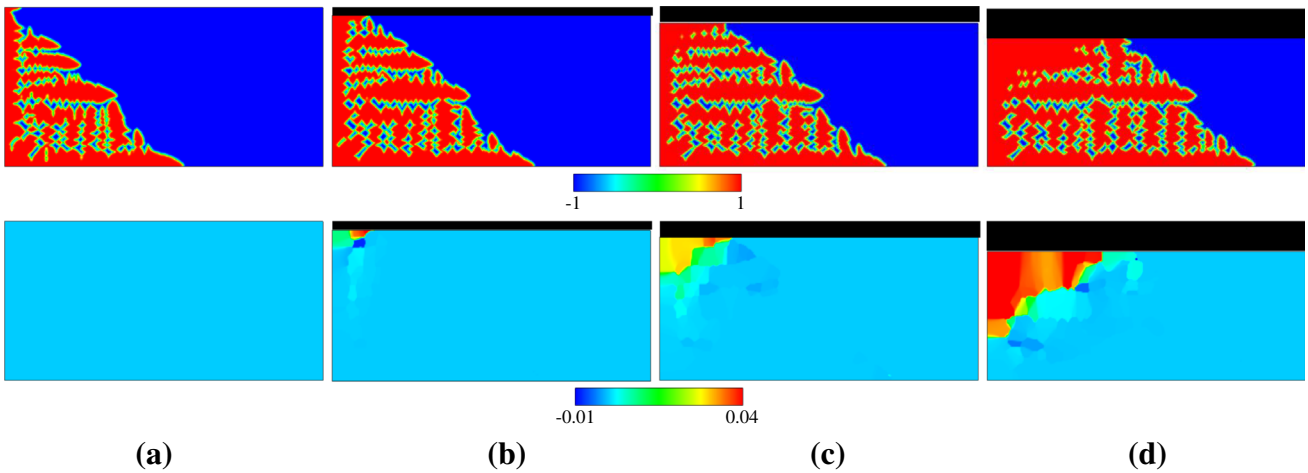

Fig. 7. Computed phase field (upper row) and crystallographic orientation angle (lower row) contours during solidification and compression of a dendritic network: (a) 0% compression, (b) 5% compression, (c) 10% compression, and (d) 20% compression.

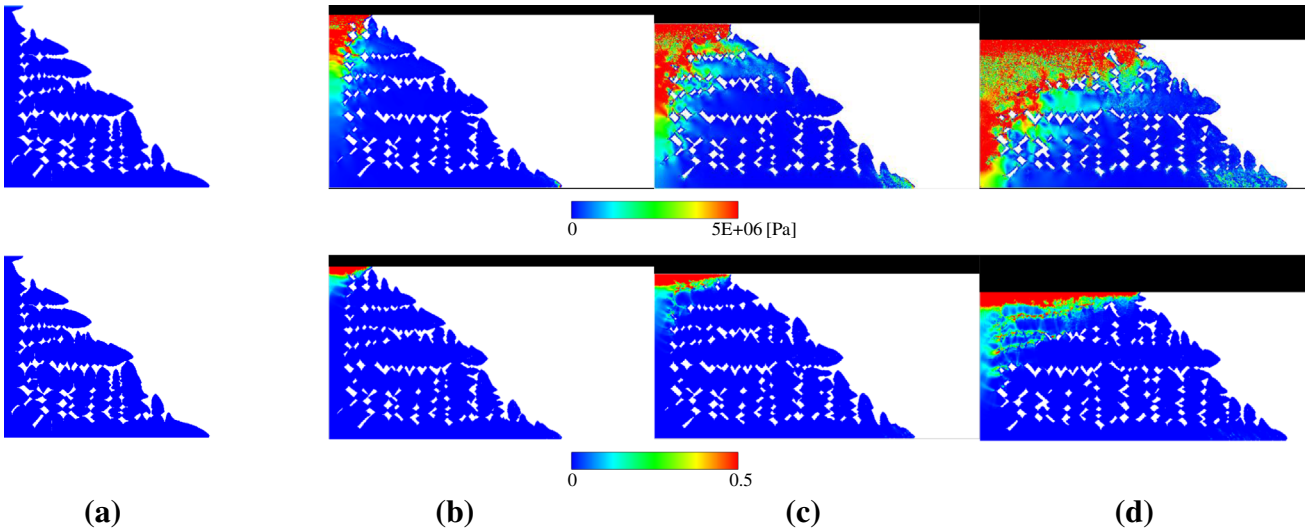

Fig. 8. Computed von Mises stress (upper row) and equivalent plastic strain (lower row) contours in the solid during solidification and compression of a dendritic network: (a) 0% compression, (b) 5% compression, (c) 10% compression, and (d) 20% compression.

Compression of a Dendritic Network

The third simulation example involves compression of a single-crystal dendritic network at a high volume fraction of solid. Initially, a single seed with $\alpha = 0$ is placed in the lower left corner of a rectangular domain with adiabatic boundaries. After some time, the vertically growing dendrite arm along the left wall reaches the upper boundary of the domain. As shown in Fig. 6, at that time a complex single-crystal dendritic network is established over much of the domain and compression is initiated. Inside of the dendritic network, the solid fraction is about 80%. During the compression, the upper domain wall is moved downward, while frictionless sliding is allowed along all other walls (Fig. 6). The compression rate is chosen such that at 20% compression, the horizontally growing dendrite arm along the lower domain wall increases in length by about 150%.

Figure 7 shows the computed phase field and crystallographic orientation angle contours at 0%, 5%, 10%, and 20% compression. The corresponding von Mises stress and equivalent plastic strain contours in the solid are displayed in Fig. 8. It can be seen that the yield stress in the solid is first reached in the upper left corner of the domain. With increasing compression, the region of plastic deformation propagates downward and to the right inside of the dendrite arms that are directly adjacent to the left vertical and upper horizontal domain walls. The compression causes some of the interior dendrite arms in the upper portion of the domain to impinge and merge. Yielding can be observed in the relatively thin rows of bridges between impinging dendrite arms. At 20% compression, a continuous, fully solid region exists in approximately the upper 25% of the solid network (upper panels of Fig. 7). On the other hand, the dendrite arms in the lower portion of the domain are essentially undeformed. The lower panels of Fig. 7 indicate that the plastic deformation of the dendritic network causes again the formation of numerous subgrains that are separated by low-angle grain boundaries. As in the previous example, these grain boundaries exist both within individual dendrite arms and between deformed dendrite arms that have impinged.

CONCLUSION AND OUTLOOK

A model has been developed to numerically simulate coupled solidification and deformation of dendritic structures. Solidification and grain boundary dynamics are modeled using the polycrystalline phase-field model of Warren et al.[12] This model is modified to account for the advection of the phase field, temperature, and crystallographic orientation angle by solid deformation. The stresses and elasto-viscoplastic strains in the solid are computed using the material point method.[13] The mechanical behavior of a grain boundary is modeled using a highly approximate procedure that is based on the local value of the phase field. Fully solid behavior is assumed when $\phi > 0$ everywhere inside of a grain boundary. Conversely, for values of $\phi < 0$, the grain boundary is assumed to contain sufficient liquid-like material that no stresses are transmitted.

Three examples are presented to demonstrate the suitability of the current model to simulate the coupled solidification and deformation of dendritic structures. The results show that complex stress and strain distributions develop in a compressed dendrite. The deformations result in variations in the crystallographic orientation angle within a single dendrite that, in turn, affect the subsequent solidification behavior. Shearing of a dendritic structure occurs primarily in relatively narrow

bands near or inside grain boundaries or the thin junctions between different dendrite arms. The deformations can cause the formation of low-angle tilt grain boundaries inside of individual dendrite arms. In addition, grain boundaries form when different arms of a deformed single dendrite impinge. During compression of a high solid fraction single-crystal dendritic structure, the deformations are limited to a relatively thin layer along the compressing boundary. The compression causes consolidation of this layer into a fully solid structure that consists of numerous subgrains.

The simulations in this article are limited to two dimensions and dendritic growth conditions that would be difficult to achieve in an experiment. These choices were made to achieve reasonable computational times (of the order of 1 day) on a standard single processor computer workstation. More realistic, three-dimensional simulations would be needed to allow for an investigation into the constitutive behavior of semisolid mushy zones in casting processes. Three-dimensional simulations are possible because three-dimensional versions of both the polycrystalline phase-field model[14] and the material point method[15] are available. However, such simulations would require large computer resources. In addition, the parameters in the polycrystalline phase-field model should be adjusted to more closely correspond to real materials.

Future work should also include modeling of the flow of the liquid surrounding the deforming solid. In this respect, it would be desirable to solve a unified, phase-field-dependent equation of motion for both the solid and the liquid. The main difficulty with such an equation would be to realistically model the transition from solid to liquid mechanical behavior inside of the diffuse interface. In the phase-field model of melt convection during solidification by Beckermann et al.,[16] the solid was assumed to be rigid and stationary so that only a liquid momentum equation needed to be considered. Sun and Beckermann[17,18] extended this model to two immiscible Newtonian fluids having large viscosity contrasts. A phase-field model for simultaneous solid deformation and liquid flow is still not available. A unified equation of motion would also need to better account for the mechanics of grain boundaries. It should take into account the dependence of the mechanical behavior of a grain boundary on the local crystalline order.

ACKNOWLEDGEMENTS

This work was financially supported, in part, by NASA under Grant Number NNX10AV35G.

REFERENCES

1. J.A. Dantzig and M. Rappaz, *Solidification* (Lausanne, Switzerland: EPFL Press, 2009).
2. M. Flemings, *Metall. Mater. Trans. B* 22, 269 (1991).
3. M.G. Pokorny, C.A. Monroe, C. Beckermann, Z. Zhen, and N. Hort, *Metall. Mater. Trans. A* 41A, 3196 (2010).
4. A.B. Phillion, S.L. Cockcroft, and P.D. Lee, *Acta Mater.* 56, 4328 (2008).
5. D. Fuloria and P.D. Lee, *Acta Mater.* 57, 5554 (2009).
6. T. Uehara, M. Fukui, and N. Ohno, *J. Cryst. Growth* 310, 1331 (2008).
7. I. Farup, J.M. Drezet, and M. Rappaz, *Acta Mater.* 49, 1261 (2001).
8. S. Terzi, *Scripta Mater.* 61, 449 (2009).
9. M. Sistaninia, A.B. Phillion, J.M. Drezet, and M. Rappaz, *Metall. Mater. Trans. A* 42A, 239 (2011).
10. M. Yamaguchi and C. Beckermann, *Acta Mater.* 61, 4053 (2013).
11. M. Yamaguchi and C. Beckermann, *Acta Mater.* 61, 2268 (2013).
12. J.A. Warren, R. Kobayashi, A.E. Lobkovsky, and W.C. Carter, *Acta Mater.* 51, 6035 (2003).
13. D. Sulsky, Z. Chen, and H.L. Schreyer, *Comput. Methods Appl. Mech. Eng.* 118, 179 (1994).
14. R. Kobayashi and J.A. Warren, *Physica A* 356, 127 (2005).
15. A. Gilmanov and S. Acharya, *Int. J. Numer. Methods Fluid* 56, 2151 (2008).
16. C. Beckermann, H.J. Diepers, I. Steinbach, A. Karma, and X. Tong, *J. Comput. Phys.* 154, 468 (1999).
17. Y. Sun and C. Beckermann, *Physica D* 198, 281 (2004).
18. Y. Sun and C. Beckermann, *Physica D* 237, 3089 (2008).